THE MESOSCALE PHYSICS OF LARGE-AREA PHOTOVOLTAICS

V. G. Karpov, Diana Shvydka,Yann Roussillon, and A. D. Compaan
Department of Physics and Astronomy, University of Toledo, Toledo, OH 43606, USA

ABSTRACT

Recent findings make the physics of large-area thin-film devices a distinctive field of its own, considerably different from that of microelectronics. We show that (i) large-area thin-film photovoltaic (PV) devices are intrinsically nonuniform in the lateral directions, (ii) the nonuniformity spans over microscopically large dimensions, which can vary dramatically (from microns to meters) depending on light intensity and bias, and (iii) the nonuniformity significantly impacts the device performance and stability. Our understanding suggests the concept of interfacial layer that blocks the nonuniformity effects and can be applied photo-electrochemically. This concept is experimentally verified.

INTRODUCTION

Because of the large-area requirements, PV thin films cannot be made crystalline and are manufactured polycrystalline or amorphous. Associated with their non-crystalline structure are lateral device nonuniformities. Technologically, nonuniformity length scales ranging from microns to tens of centimeters can originate from different process steps [1,2] We emphasize that the processes involved (deposition, wet treatments, etc.) are intrinsically nonuniform and thus lateral inhomogeneities of the material parameters in large-area, thin-film devices are unavoidable.

Physically, the device lateral nonuniformities originate from relatively weak local fluctuations in the material structure parameters: grain size, chemical composition, etc., which translate into strong fluctuations in the electronic properties. The amplification comes from the presence of potential barriers. Indeed, electronic transport through the barriers is exponentially sensitive to the local parameter fluctuations in both the temperature-activated and tunneling modes. More specifically, for barrier of height V_B and width a, the corresponding barrier transmission probabilities, $\exp\left(-V_B/kT\right)$ and $\exp\left(-2a\sqrt{2mV_B}/\hbar\right)$ typically have exponents much greater than one. Hence, their relatively small variations cause significant effects.

The barriers in PV cells are associated with the device junctions (p-n, semiconductor/TCO, and semiconductor /metal) and grain boundaries. We show that lateral nonuniformities are observed in all major PV and that the physics of lateral nonuniformities is determined by mesoscopic length scale, $L \sim 1\ \mu m$ to 1 m.

SURVEY OF EXPERIMENTAL DATA

The nonuniformities show up in OBIC, EBIC, PL, and STM mapping and in variations between J-V parameters of nominally identical devices. We briefly review the data for major devices.

For Cu(In,Ga)Se$_2$ polycrystalline device, lateral variations in local microscopic open-circuit voltage V_{OC} ranging from 0.2 to 0.7 V were detected by STM [3] and OBIC measurements revealed microregions of reduced photovoltaic efficiency [4].

For CdS/CdTe polycrystalline PV cells, OBIC [5] and EBIC [6,7] showed strong inhomogeneities dependent on postdeposition treatments with length scales ranging from microns to millimeters [8]. Time-resolved PL in CdS/CdTe solar cells revealed variations in recombination lifetime [9]. PL mapping [10] showed nonuniformities whose topology depends on the excitation power. Scanning ballistic electron emission spectroscopy revealed the barrier height dispersion of ~0.1 eV in a crystalline CdTe/metal junction [11,12]. Mapping of a polycrystalline CdTe cell fabricated with a high resistance contact [13] showed ~ 0.2 eV electric potential variations. It was found that lateral nonuniformities cause variations between PV parameters of nominally identical cells [14]. Nonuniform degradation in CdTe cells was noticed in Refs. [1,15,16].

For a-Si:H, changes in photoinduced degradation, defect density and PV parameters were found to depend on nano- and longer length scales of structural inhomogeneity [17,18]. Lateral nonuniformities in V_{OC}, short-circuit current j_0 and other parameters were identified in micro-, multi-, and polycrystalline silicon [19,20,21]. Local sites of diode nature, different from the standard ohmic shunts, dominated forward current through a multi-crystalline cell [22, 23].

Schottky diodes have proven to be inhomogeneous even when based on crystalline semiconductors [24, 25, 26, 27]. This implies again that barrier-controlled transport is exponentially sensitive to local fluctuations in material parameters. Existing theories attribute such fluctuations either to electric charge density [28] or defect concentration that affect the barrier tunneling transparency [29]. Highly nonuniform charge flow induced by ionized defects evidenced also in the pitted submicron morphology obtained by photoetching [30].

We conclude that major photovoltaic devices are intrinsically nonuniform in the lateral directions and that the nonuniformity length scales can vary in a broad range from microns (individual grains) to meters (manufacturing deposition scales).

MODEL

Understanding of lateral fluctuations lies in the device diode nature and in the presence of the resistive electrode [1,13,15]. This is reflected in the equivalent circuit of random microdiodes connected in parallel through the resistive electrode. The ideal diode model approximates each microdiode,

$$j = j_0 \left\{ \exp\left[\frac{e(V - V_{oc})}{kT} \right] - 1 \right\} \quad . \qquad (1)$$

The microdiode size is of the order of the nonuniformity length scale l. The effects of lateral micrononuniformities depend on the relationship between l and the screening length [13, 31] L,

$$L = \sqrt{u / \rho j_0} \quad , \qquad (2)$$

where u is the local fluctuation of electric potential. The physical meaning of L is that the fluctuation u is balanced by the potential drop $j_0 L^2 \rho$ across the lateral resistance. This applies to both the one-dimensional (D=1) and two-dimensional (D=2) case. For D=1, ρL and $j_0 L$ represent the resistance and current, and ρ is the resistance per unit length. For D=2, the resistance is represented by the sheet resistance ρ and the current is $j_0 L^2$.

The maximum screening length corresponds to a dead shunt ($u = V_{OC}$). The minimum screening length L_0 is defined by Eq. (2) with $u = kT/e$. L varies over a wide range depending on the sheet resistance and photocurrent. For example, $\rho \sim 10\ \Omega/\square$ for the typical transparent conductive oxide used as a contact. This gives $L_0 \sim 1\text{mm}$ under 1 sun illumination while under ambient room light it can be as large as 1 m. For a non-metallized device using the semiconductor sheet resistance reduces L down to $L \sim 1\ \mu\text{m}$.

Eq. (2) describes a system with a single weak diode. For multiple random diodes with size $l \gg L$ the neighboring units are electrically insulated. The observed quantities then correspond to a locally tested microdiode. In particular, L sets the upper limit to the size of an efficient cell.

Given the range of L from $\sim 1\text{mm}$ to $\sim 1\text{m}$ and the much shorter fluctuation length scale l ($\sim 1\mu\text{m}$), the opposite limiting case of interacting microdiodes, $l \ll L$ is practically important, which is discussed in Refs. [1,13, 15]. An important entity is a weak (low V_{OC}) diode. It finds itself under forward bias u and robs currents from a large number $(L/l)^D \gg 1$ of more robust neighbors. Such non-ohmic shunting does not affect the performance in reverse bias.

When there are several equally weak diodes in the region of the length L, the correlation radius R, whose standard meaning is that the system is uniform on length scales longer than R, becomes a relevant length. Because the number of significantly different microdiodes in the system is $e\Delta/kT$, where Δ is the characteristic width of the

V_{OC} distribution, one can estimate $R = l(e\Delta/kT)^{1/D}$. Typically, $R \ll L$.

The multi-diode circuit can be simulated by numerically solving the corresponding Kirchhoff's equations for a given random input parameter distribution. The calculated output parameter distributions show indeed that weak microdiodes force strong currents of the polarity opposite to that of the majority of diodes (Fig. 1).
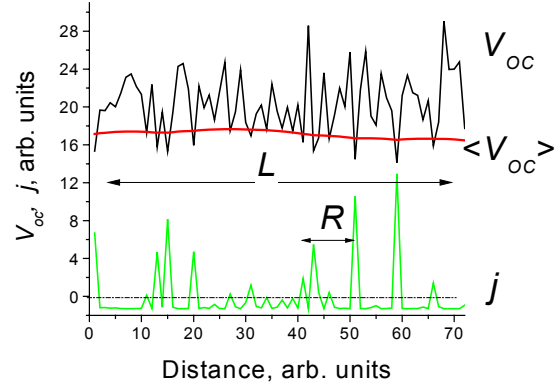
Fig. 1. Simulated open-circuit voltage (V_{OC}) and transverse electric current (j) distributions in an open-circuit system of random diodes. Rare strong positive currents correspond to weak diodes balancing the majority of robust diode currents, which are negative. Note that the robust diode negative currents are practically the same as they would be under short-circuit conditions. The correlation radius (R) and the weak diode screening length (L) are also shown.

For $N \gg 1$ diodes occupying a volume of linear dimension $x \ll L$, but still macroscopically uniform ($x \gg R$), the resistive potential drop across the domain is small and the diodes are under almost the same potential $\langle V_{OC} \rangle$. The latter can be found by setting to zero the sum of N random currents (under open-circuit conditions), each given by Eq. (1),

$$\langle V_{OC} \rangle = -\frac{kT}{e} \ln \left\langle \exp\left(-\frac{eV_{OC}}{kT} \right) \right\rangle_N \qquad (3)$$

Since the balance of currents (rather than V_{OC}) determines the average macroscopic potential, the weak diode contribution is exponentially significant, that is the device open-circuit voltage is strongly reduced by relatively small concentration of weak diodes. As an illustration, in a system of 100 diodes, one weak diode with V_{OC} by 0.3 V lower than its neighbors' decreases the measured V_{OC} by 0.2 V at room temperature.

One can also say that the recombination of photogenerated electrons occurs mostly through weak diodes, as opposed to the ideal system where it is spatially uniform. The degree of nonuniformity in V_{OC} needed to make the difference is as low as several kT/e (~ 0.1 V at room temperature), well within the observed range of the V_{OC} fluctuation data.

BLOCKING NONUNIFORMITIES

Here we introduce one remedy, which, while keeping the semiconductor structure intact, can significantly level out the device nonuniformity. Our consideration predicts that because the surface photovoltage varies across the film, electrochemical treatments will act differently on different spots (Fig. 2). When properly chosen they should selectively deposit 'clogs' onto the weak diode spots thus eliminating the most significant sources of nonuniformity. In other words, we predict nonuniformity self-healing by photo-electrochemical treatments. The result of such treatment will be an interfacial layer (IFL), whose expected properties are higher degree of device uniformity and higher V_{oc}.

We verified this prediction experimentally by using treatments that combine the features of electrolyte and colloidal suspension; the latter aimed at better clogging weak spots. Red wine represents one such characteristic and curious example. Indeed, shown in Fig. 3 the J-V characteristics are markedly different for the cases of untreated, dark-treated, and light-treated samples. Another, more "scientific" treatment was a solution based on aniline in p-toluenesulphonic acid, which causes a significant improvement as applied under the light for 30 min and is much less effective as applied in the dark.
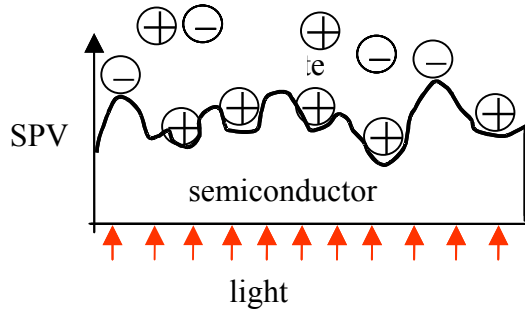

Fig. 2. Sketch of the experimental setup of selective photo-electrochemical treatment. The fluctuating surface photovoltage (SPV) corresponds to the CdTe surface of a CdS/CdTe polycrystalline cell.

In chemically designing the electrolyte composition it is important to understand the role of nonuniformity screening length, which in the absence of metal, is dominated by the electrolyte resistivity r (Ω-cm). Reasoning along the same lines as in deriving Eq. (2), one can obtain

$$L = \frac{u}{j_0 r} \quad . \tag{4}$$

In order to effectively level out the device nonuniformity, the inequality $L \gg l$ should obey where L is given by Eq. (4).

It is likely that in some cases treatments of the above kind have already been found by trial and error. In particular, our results in Fig. 3 are similar to the published data on the interfacial layer effects [2] that while used in production remained poorly understood. That might also explain why different pre-contact treatments, including weak etches, exposure to organics, even varying ambient atmosphere conditions have a profound effect on device parameters. We believe that our present consideration provides the understanding to search effectively for the desired treatments.
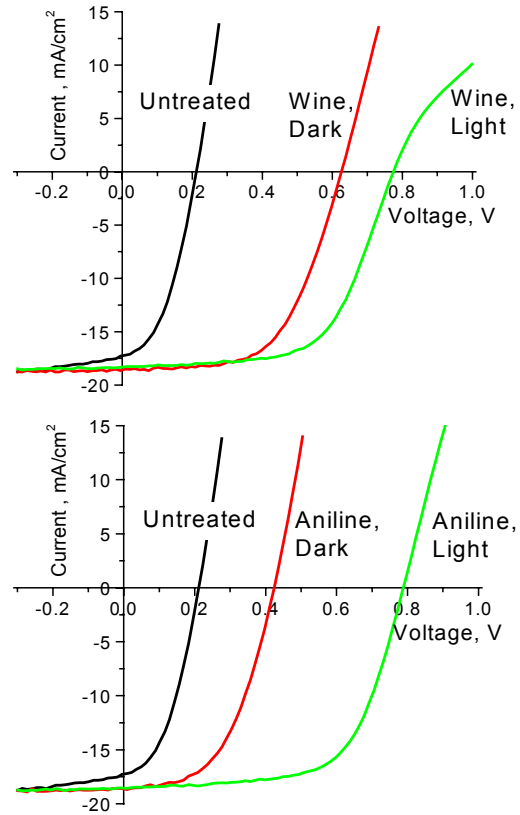
Fig. 3. Effect of electrolyte surface treatments and light exposure on J-V curves: *top* - red wine, *bottom* - aniline solution. CdS/CdTe samples were made by vapor transport deposition as described in [2, 7].

CONCLUSIONS

In conclusion, we have shown that large-area semiconductor devices are intrinsically nonuniform, which makes their physics qualitatively different from that of microelectronics. The nonuniformity length scales cover a broad spectrum ranging from microns to meters. They show up in different types of experiments and for the major thin-film semiconductor devices.

We have also found a characteristic screening length that ranges from millimeters to meters and explains how a microscopic nonuniformity can affect macroscopically large areas in the film. A theoretical model of random diodes

explained some of the observed features. Our consideration here has suggested an interfacial layer concept of overcoming these nonuniformity effects and self-healing photo-electrochemistry approach to depositing the required layer.

Another closely related application where the concepts of nonuniformity and random diode arrays can be extremely important is the macroscopic circuitry of large area PV modules and their field arrays. A typical PV module is composed of a large number (~ 100) of linear cells *in series*. Because of the cell diode nature, these series will be very sensitive to small variations in the cell parameters; hence, the problem of random diodes in series. Furthermore, in the field, PV arrays form more complex circuits where, for example, blocks of many modules in parallel are connected in series. Again, since the modules have slightly different characteristics, the latter systems will belong to the class of random diode systems. A relevant theoretical approach is needed to understand their physics and optimize the design.

REFERENCES

[1] V. G. Karpov, A. D. Compaan, and D. Shvydka. *Proceedings of 29th Photovoltaic Specialists Conference*, (IEEE, New Orleans, 2002) p. 708.

[2] D. Rose, R. Powell, U. Jayamaha, M. Maltby, *Proceedings of 29th Photovoltaic Specialists Conference*, (IEEE, New Orleans, 2002) p. 555.

[3] D. Eich, U. Hereber, U. Groh, U. Stahl, C. Heske, M. Marsi, M. Kiskinova, W. Reidl, R. Fink, E. Umbach, *Thin Solid Films* **361**-**362**, p. 258 (2000).

[4] G. A. Medvedkin, L. Stolt and J. Wennerberg, *Semiconductors* **33**, p. 1037 (1999).

[5] S. A. Galloway, A. W. Brinkman, K. Durose, P. R. Wilshaw, and A. J. Holland, *Appl. Phys. Lett.* **68**, p. 3725 (1996).

[6] P. R. Edwards, S. A. Galloway, and K. Durose, *Thin Solid Films* **372**, p. 284 (2000).

[7] R. Harju, V. G. Karpov, D. Grecu, G. Dorer, *J. Appl. Phys.* **88**, p. 1794 (2000).

[8] P. N. Gibson, M. A. Baker, E. D. Dunlop, M. E. Ozsan, D. Lincot, M. Froment, G. Agostinelli, *Thin Solid Films* **387**, p. 92 (2001).

[9] R. K. Ahrenkiel, B. M. Keyes, D. L. Levi, K. Emery, T. L. Chu, and S. S. Chu, *Appl. Phys. Lett.* **64**, p. 2879 (1994).

[10] Diana Shvydka, A. D. Compaan and V. G. Karpov, *J. Appl. Phys.* **91**, p. 9059 (2002).

[11] I. M. Dharmadasa, C. J. Blomfield, C. G. Scott, R. Coratger, F. Ajustron, and J. Beauvillain, *Solid State Electronics* **42**, p. 595 (1998).

[12] C. F. Alonso, M. P. Hernandez, E. Cassielles, and J. L. Pena, *Appl. Phys. Lett.* **80**, p. 3751 (2002).

[13] V. G. Karpov, R. Harju, and G. Dorer, *Proceedings of 28th Photovoltaic Specialists Conference*, (IEEE, Alaska, 2000), p. 547.

[14] D. Shvydka, A. D. Compaan, and V. G. Karpov, *Appl. Phys. Lett.* **82**, p. 2157 (2003).

[15] V. G. Karpov, A. D. Compaan, and Diana Shvydka, *Appl. Phys. Lett.* **80**, p. 4256 (2002).

[16] A.O. Pudov, M. Gloeckler, S.H. Demtsu, and J.R. Sites, K.L. Barth, R.A. Enzenroth, and W.S. Sampath, *Proceedings of 29th Photovoltaic Specialists Conference*, (IEEE, New Orleans, 2002) p. 760.

[17] N. Sakikawa, M. Tamao, S. Mayazaki, and M. Hirose, *Jpn. J. Appl. Phys.* **37**, p. 432 (1998); *ibid.*, **38** p. 5768 (1999).

[18] U. K. Das, J. K. Rath, D. L. Williamson, and P. Chaudhuri, *Jpn. J. Appl. Phys.* **39**, p. 2530 (2000).

[19] R. Baldner, H. Lautenschlager, C. Schetter, R. Schindler, W. Warta, *Proceedings of 25th Photovoltaic Specialists Conference*, (IEEE, Washington DC, 1996) p. 641.

[20] I. Tarasov, S. Ostapenko, and J. P. Kalejs, *Proceedings of 28th Photovoltaic Specialists Conference*, (IEEE, Alaska, 2000) p. 112.

[21] J. P. Boyeaux, A. Kaminski, N. Ferrer, S. Berger, and A. Laugier, *Proceedings of 28th Photovoltaic Specialists Conference*, (IEEE, Alaska, 2000) p. 319.

[22] I. E. Konovalov, O. Breitenstein, and K. Iwig, *Sol. Energy Mater. Sol. Cells* **48**, p. 53 (1998).

[23] O. Breitenstein and M. Langenkamp, *2nd World Conference on photovoltaic solar energy conversion*, Vienna, Austria (1998), p. 1382.

[24] Kh. G. Naghmudinov and T. A. Polyanskaya, *Sov. Phys. Semicond.* **21**, p. 1053 (1987).

[25] L. E. Calvet, R. G. Wheeler, and M. A. Reed, *Appl. Phys. Lett.* **80**, p. 1761 (2002).

[26] W. Monch, *J. Vac. Sci. Technol.* **17**, p. 1867 (1999).

[27] H.–J. Im, Y. Ding, J. P. Pelz, W. J. Choyke, *Phys. Rev. B* **64**, p. 075310 (2001).

[28] R. T. Tung, *Appl. Phys. Lett.* **58**, p. 2821 (1992).

[29] M. E. Raikh and I. M. Ruzin, in: *Mesoscopic Phenomena in Solids*, Edited by B. L. Altshuller, P. A. Lee, and R. A. Webb, Elsevier (1991), p. 315.

[30] R. Tenne, V. Marcu, and N. Yellin, *Appl. Phys. Lett.* **45**, p. 1219 (1984).

[31] V. G. Karpov, G. Rich, A. V. Subashiev, and G. Dorer, *J. Appl. Phys.* **89**, p.4975 (2001).